Site-Specific Neutralization of Low Energy $^7Li^+$ Scattered from Na/Al(100)

K. A. H. German,[1,2] C. B. Weare,[1,2] P. R. Varekamp,[1] J. N. Andersen,[3] and J. A. Yarmoff[1,2]

[1]*Department of Physics, University of California, Riverside, California 92521*

[2]*Materials Sciences Division, Lawrence Berkeley Laboratory, Berkeley, California 94720*

[3]*Department of Synchrotron Radiation Research, Institute of Physics, Lund University, Sölvegatan 14, S-223 62 Lund, Sweden*

(Received 4 September 1992)

Site-specific neutralization is seen for low energy (1–5 keV) $^7Li^+$ ions scattered at large angles from Na-covered Al(100). Energy spectra of the ion yield are collected near the surface normal as a function of Na coverage. Li^+ singly scattered from Na is almost completely neutralized, while the neutralization of ions scattered from Al is fairly insensitive to coverage, indicating a large difference in the local electrostatic potential above Na and Al sites. This shows that the phenomena of resonant charge exchange is capable of resolving atomic scale variations in the surface potential.

PACS numbers: 79.20.Rf, 34.70.+e, 79.90.+b, 82.65.My

While it is well established that the ion fractions of alkalis scattered from surfaces are sensitive to the decrease in work function induced by alkali adsorption, it has not been previously shown that different neutralization rates can be correlated with short order variations in the local electrostatic potential of an alkali-covered metal surface. This work represents the first direct observation of different neutralization rates for alkali atoms scattering from different atomic sites of the same surface. The observed neutralization behavior directly demonstrates that the phenomena of resonant charge neutralization is capable of resolving variations in the local electrostatic potential on an atomic scale.

In alkali ion scattering, the s level of the projectile interacts with the surface so as to allow an electron to resonantly tunnel between the projectile's s level and the Fermi level of the surface. Since tunneling is a reversible process, the final charge state of a scattered alkali is established along the particle's exit trajectory. Because the electron affinity of an alkali ion is comparable to the work function of a surface, the ion fraction of a scattered alkali ion beam is strongly dependent on the work function. As a consequence of this dependence, it is found that the scattered alkali ion fraction decreases with increasing alkali coverage. While it is relatively easy to measure an increase in resonant neutralization as a function of alkali coverage [1–3], it is considerably more difficult to detect the more subtle effects that a nonuniform surface local electrostatic potential has on the neutralization probabilities.

The present work employs 1 to 5 keV Li^+ ions incident along the surface normal. Backscattered ions are detected and energy analyzed at an angle of $11.6° \pm 0.5°$ from the surface normal. By scattering with an exit trajectory near the surface normal, the geometrical and theoretical complications associated with motion parallel to the surface are removed, which allows the measured ion yield to be directly correlated with the electrostatic potential at a particular surface site.

The survival probability of a given species undergoing resonant neutralization depends on the electrostatic potential that the projectiles experience as they leave the surface, and on motion both parallel and perpendicular to the surface. Although the quantitative analysis of these dependencies is quite complex, a major complication of parallel motion can be understood qualitatively as illustrated in Fig. 1, within the context of the semiclassical model [4]. This model assumes that the final charge state is established at a "freezing distance," z^*, from the surface. In Fig. 1, the off-normal scattering geometry is seen to obscure the association of the local electrostatic potential with a particular scattering site since the scattered ions will traverse z^* at a location that is laterally displaced from the scattering site. On the other hand, the neutralization of ions leaving near the surface normal is determined by the local electrostatic potential immediately above the scattering site. Since freezing distances are comparable to nearest-neighbor lattice spacings, typically 2–5 Å, the use of an off-normal geometry destroys the correlation between the scattering site and the ion fraction, even if the exit trajectory has a fairly large component perpendicular to the surface. The degradation of

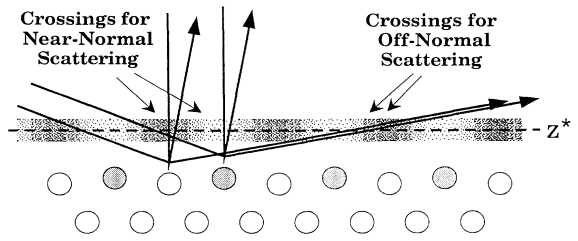

FIG. 1. Schematic of near-normal scattering and grazing angle scattering through an inhomogeneous local electrostatic potential above an alkali-covered metal. The freezing distance is illustrated by the hatched line labeled z^*. Ion trajectories are depicted by bold arrows. The variegated shading represents the corrugated local electrostatic potential at z^*.

the correlation between a neutralization rate and the potential at a scattering site due to thermal vibrations and defects is also exacerbated by parallel motion. Furthermore, since the freezing distance increases as the velocity perpendicular to the surface decreases, the neutralization behavior associated with an off-normal trajectory will correspond to the local electrostatic potential further away from the surface as compared to those leaving the surface with the same energy along the surface normal. The net effect is that the data collected at grazing angles [1,5] are best modeled by assuming a uniform work function and including the Galilean transformation required to account for the effects of parallel motion on the resonant tunneling process [6].

The experiments were performed in an ultrahigh vacuum (3×10^{-11} torr) chamber equipped with a $^7Li^+$ ion gun (Kimball Physics) that produces a beam with a spot size of <1 mm^2, a sputter gun used for sample cleaning and He^+ ion scattering, and a spherical electrostatic energy analyzer (Comstock). Scattered ions were detected at a scattering angle of $\Psi=168.4°$ for Li^+ and $\Psi=158°$ for He^+. Energy spectra were collected at room temperature (RT) with 1 to 5 keV $^7Li^+$ and 1 to 2 keV $^4He^+$ ions. The Al(100) sample was cleaned by reiteratively sputtering with 1 or 0.5 keV Ar^+ at 300 °C and annealing to 450 °C. A well-outgassed SAES getter was used for Na deposition. The purity and order of the surface were verified using Auger electron spectroscopy (AES) and low energy electron diffraction (LEED). To insure that sample damage due to the ion beam did not affect the results, each spectrum was taken at a different region of a newly cleaned and prepared sample, and the ion flux was reduced so that consecutive scans taken from the same region were indistinguishable. Na coverages on the Al(100) surface ranged from less than 0.01 monolayer (ML) to the 0.5 ML coverage associated with a $c(2\times2)$ LEED pattern [7]. Coverages were estimated by assuming a constant sticking coefficient [7], and using the appearance of the sharpest $c(2\times2)$ LEED pattern as a calibration.

Several energy spectra are shown in Fig. 2 for normal incidence 2.93 keV $^7Li^+$ and 2 keV $^4He^+$ scattered from clean Al(100) and Al(100) with various Na coverages. AES spectra taken before and after each run verified that O contamination remained at $<0.1\%$ of a ML. In Fig. 2, the Li^+ spectra are all plotted on the same scale with no offset. Signal averaging of spectra collected from different regions of the sample was employed to improve the signal-to-noise ratio without inducing further beam damage. Data from different runs were normalized to the clean surface spectrum from each individual run in order to correct for any long term drift in the sensitivity of the analyzer. The 2 keV He^+ spectra collected from the clean and $c(2\times2)$ surfaces are shown in Fig. 2 normalized to equal peak area. Note that spectra collected with other incident beam energies (not shown) display nearly identical behavior.

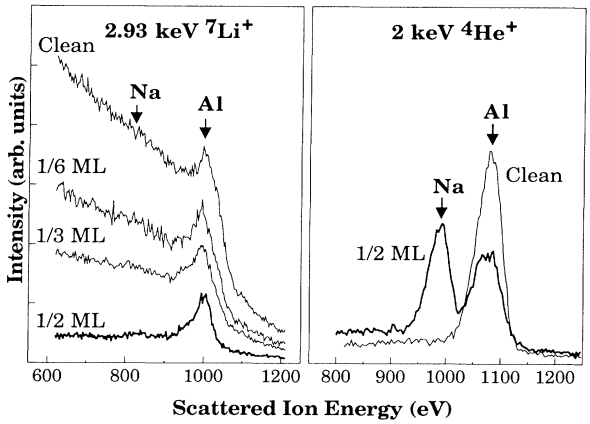

FIG. 2. Scattered ion energy spectra collected at normal incidence for 2.93 keV $^7Li^+$ and 2 keV $^4He^+$ scattered from clean Al(100) and after various Na exposures. The single scattering energies for Na and Al are indicated. The spectra shown in bold were collected from the same surface, which had a Na coverage of 0.5 ML and displayed a sharp $c(2\times2)$ LEED pattern.

The energy distribution of the scattered ions distinguishes between multiple and single scattering, and between ions singly scattered from different species. Single scattering produces peaks at energies that are directly correlated to the mass of the target atom. The Na and Al single scattering peaks are indicated in Fig. 2. Note that the energy of the single scattering peak is ~25 eV lower than predicted by the binary collision approximation due to inelastic effects [8]. The Li^+ spectra of the clean surfaces are characterized by a single scattering peak on top of a multiple scattering background. As Na is deposited, there is a substantial overall reduction in the ion backscattering yield as well as a change in the shape of the spectra.

Remarkably, no sizable $^7Li^+$ single scattering from Na is seen for any of the Na-covered surfaces, while at the same time He^+ scattering shows that Na is present on the top layer. Because He^+ ions neutralize via an irreversible Auger process, which is a steep function of depth penetrated, there is little multiple scattering signal in the He^+ spectra [9]. The comparable intensity of the He^+ single scattering peaks from Na and Al reflects the fact that one-half of a ML of each species is present in the outermost surface layer. The Na signal is slightly larger than the Al signal because the Na atoms are positioned above the outermost Al atoms.

In the absence of neutralization, the intensity of the Li^+ single scattering from Na at the $c(2\times2)$ coverage would be nearly one-third of that from Al for the following reasons. At normal incidence on an fcc (100) surface, the first two atomic layers are directly visible to the incident ion beam, while the deeper layers are shadowed

by the first two layers. Thus, the first two atomic layers are responsible for all of the observed single scattering signal from the clean surface. At the $c(2\times2)$ coverage, however, adsorbed Na shadows half of a ML of either first or second layer Al, depending on whether the adsorption site is atop, fourfold hollow, or substitutional. The difference in cross section for scattering from Na and Al is small; i.e., the ratio of the partial cross sections for 3 keV Li^+ to scatter through 168° from Na as compared to Al is 0.89. Calculations of shadowing and blocking events show that there is no enhancement of the Al signal due to focusing at this orientation [10], which has been experimentally verified by analysis of polar angle scans collected from this same system [11]. The fact that the Na signal is much smaller than $\frac{1}{3}$ of the Al signal thus proves that ions scattered from Na are preferentially neutralized.

The anomalous neutralization behavior of Li^+ scattered from Na-covered Al(100) is a direct consequence of alkali adsorbate-induced variations of the surface local electrostatic potential. The total neutralization of Li^+ scattering from Na is due to a relatively low electrostatic potential above the adsorbate, while scattering from Al is always observed because the local electrostatic potential is higher above Al sites than above Na sites.

The change in shape of the spectra further supports this interpretation. The multiple scattering signal is due to ions that leave the surface from regions extending over the entire surface area. The fact that the multiple scattering signal decreases more rapidly than the Al single scattering signal indicates that the local electrostatic potential above the majority of the surface decreases more rapidly than the potential directly above the Al sites. The changes to the multiple scattering background also confirm that the ion fraction is extremely sensitive to work function changes. For example, even for coverages of less than 0.01 ML, a drop in the multiple scattering signal of $\sim 15\%$ is observed.

The fact that the intensity of the single scattering peak does not decrease as rapidly as the multiple scattering signal is further testimony as to the degree of inhomogeneity in the local electrostatic potential of this system. Indeed, the intensity of the single scattering peak above the multiple scattering background remains nearly constant throughout the coverage regime shown here. This is remarkable, especially considering the expected decrease in Al single scattering due to shadowing, as discussed above. The strong persistence of the Al single scattering peak indicates that the local electrostatic potential above Al sites is largely unaffected by the presence of Na in this coverage regime. This observation gives an indication of the magnitude of the variations in the surface potential. For example, at the $c(2\times2)$ coverage, the average work function has decreased from 4.4 to 2.8 eV [12]. If the potential at the Al sites is only slightly affected, then the potential at the Na sites must be considerably less than 2.8 eV.

In light of the results presented here, it is useful to consider other work done on Na/Al systems. Published calculations show that upon adsorption of Na on Al(100) at fourfold hollow sites, electron charge density leaves the neutral Na atom and accumulates between the adsorbate and the Al surface [13,14]. If the calculated charge density distributions are accurate, then the local electrostatic potential above the surface should reflect changes in the intensity and contour of the Na-induced dipole layer. What is surprising is that the calculations in Ref. [14] for the $c(2\times2)$-Na/Al(100) surface show a nearly uniform dipole layer, which would produce roughly equal neutralization rates for the Na and Al single scattering peaks, in contradiction to the present results. This inconsistency may, however, simply reflect an inappropriate choice of surface geometry for Na adsorbed at RT.

The effect of the surface geometry on the electron density distribution has been calculated for the $(\sqrt{3}\times\sqrt{3})$-$R30°$-Na/Al(111) surface [15]. Reference [15] contains calculated electron density distributions both for a threefold hollow adsorption site geometry and for a substitutional adsorption site. It is found that the substrate electron density between Na atoms is much larger for the substitutional geometry. This excess electron density screens the Na-Na interaction and creates a highly corrugated electron density at the surface. In other words, the surface dipole layer, and consequently the local electrostatic potential, is much more varied along the surface plane for substitutional adsorption than for adsorption at a hollow site. The difference in charge distribution between the two adsorption sites is primarily a reflection of the surface geometries rather than the nature of the adsorbate-substrate bond. If the Na atoms sit above the surface, as in a hollow site geometry, a nearly uniform plane of constant potential is formed. In a substitutional geometry, on the other hand, the surface plane alternates between Na and Al atoms, and therefore the potential is more highly corrugated.

Similarly, a substitutional geometry for Na/Al(100) is quite likely to induce an irregular charge rearrangement, and consequently produce the large differences in the Li^+ ion fractions observed for scattering from Na and Al sites. It is known that for Na on Al(111), the threefold site adsorption is observed at low temperatures, while a substitutional geometry is observed at RT [16,17]. Likewise, there is evidence that the structure of Na on Al(100) is also temperature dependent. Namely, both the behavior of the work function as a function of coverage [12] and the Al $2p$ and Na $2p$ core level shifts measured by photoemission [18] are different at 100 K and RT.

With the addition of our results, the current body of work on Na/Al systems supports a picture in which the adsorption of Na on Al(100) is at a fourfold hollow site at low temperatures and substitutional at RT. This is an

example of how the capability of detecting variations in the local electrostatic potential by employing alkali ion scattering in the present configuration can make an important contribution to the understanding of alkali-covered metal surfaces. Note that the K/Al(100) system displays temperature-dependent behavior similar to Na/Al(100) [18], also suggesting substitutional adsorption of K at RT. This is supported by our recent Li^+ ion scattering experiments on K/Al(100), which demonstrate the same highly selective neutralization behavior as the Na/Al(100) system [10].

The work reported here represents substantive improvements over previous alkali ion scattering studies which investigate the surface local electrostatic potential. First of all, the experiments reported in Refs. [1], [2], and [3] did not detect ions exiting near the surface normal. In addition, none of these experiments was designed to monitor scattering from the adsorbate and the substrate independently. Reference [1] measured the total ion fraction without any energy discrimination, and the experiments in Refs. [2] and [3] were configured such that ions scattered from the adsorbate were either at too low of an energy to detect or the adsorbate peak coincided with a strong double scattering peak from the substrate.

In the Li^+ scattering from Cs-covered Cu(110) reported by Ashwin and Woodruff [19], both the adsorbate and substrate peaks were monitored at 17° from the surface normal, but the single scattering peak from Cs was too large to conclude that any preferential neutralization had occurred. It is possible that trace amounts of O were present on their surfaces, as recent work by Jiang, Li, and Koel [5] shows that O contamination enhances the Cs signal for Li^+ scattered from Cs/Ni(111) surfaces. In addition, in our preliminary investigations of Li^+ scattering from K/Al(100) surfaces, single scattering from K is observed only in the presence of trace amounts of O [10].

The work of Ref. [5], which was collected at 18° from the normal, also confirms our result that site-specific neutralization can be detected by scattering near the surface normal. For the Cs/Ni(111) system, however, a substantial decrease in the substrate single scattering signal takes place as a function of coverage. It is likely that this reduction is a manifestation of a more uniform local electrostatic potential above Cs/Ni(111) as compared to Na/Al(100).

The results presented here show that atomic scale variations in the surface electrostatic potential can be investigated via the neutralization behavior of alkali ions scattered in a direction near the surface normal. In particular, for Na/Al(100), while the potential at the Na sites is low enough to produce nearly complete neutralization of scattered Li^+, the potential at the Al sites is only slightly modified by the presence of Na.

[1] J. J. C. Geerlings, L. F. T. Kwakman, and J. Los, Surf. Sci. **184**, 305 (1987).
[2] G. A. Kimmel, D. M. Goodstein, and B. H. Cooper, J. Vac. Sci. Technol. A **7**, 2186 (1989).
[3] G. A. Kimmel, D. M. Goodstein, Z. H. Levine, and B. H. Cooper, Phys. Rev. B **43**, 9403 (1991).
[4] J. J. C. Geerlings, J. Los, J. P. Gauyacq, and N. M. Temme, Surf, Sci. **172**, 257 (1986).
[5] L. Jiang, Y. D. Li, and B. E. Koel, Phys. Rev. Lett. **70**, 2649 (1993).
[6] R. Zimny, Surf. Sci. **233**, 333 (1990).
[7] J. O. Porteus, Surf. Sci. **41**, 515 (1974).
[8] Th. Fauster, Vacuum **38**, 129 (1988).
[9] See discussion in D. P. Woodruff and T. A. Delchar, *Modern Techniques of Surface Science* (Cambridge Univ. Press, Cambridge, 1986).
[10] K. A. H. German, C. B. Weare, and J. A. Yarmoff (to be published).
[11] K. A. H. German, C. B. Weare, P. R. Varekamp, J. A. Yarmoff, and J. N. Andersen, J. Vac. Sci. Technol. A (to be published).
[12] J. Paul, J. Vac. Sci. Technol. A **5**, 664 (1987).
[13] M. Scheffler, C. Droste, A. Fleszar, F. Máca, G. Wachutka, and G. Barzel, Physica (Amsterdam) **172B**, 143 (1991).
[14] H. Ishida and K. Terakura, Phys. Rev. B **38**, 5752 (1988).
[15] J. Neugebauer and M. Scheffler, Phys. Rev. B **46**, 16067 (1992).
[16] J. N. Andersen, M. Qvarford, R. Nyholm, J. F. v. Acker, and E. Lundgren, Phys. Rev. Lett. **68**, 94 (1992).
[17] A. Schmalz, S. Aminpirooz, L. Becker, J. Haase, J. Neugebauer, M. Scheffler, D. R. Batchelor, D. L. Adams, and E. Bøgh, Phys. Rev. Lett. **67**, 2163 (1991).
[18] J. N. Andersen, E. Lundgren, R. Nyholm, and M. Qvarford, Phys. Rev. B **46**, 12784 (1992).
[19] M. J. Ashwin and D. P. Woodruff, Surf. Sci. **244**, 247 (1991).